No. 666 **July 2023**

FEM SIMULATIONS FOR NONLINEAR MULTIFIELD COUPLED PROBLEMS: APPLICATION TO THIXOVISCOPLASTIC FLOW

N. Begum, A. Ouazzi, S. Turek

ISSN: 2190-1767

FEM SIMULATIONS FOR NONLINEAR MULTIFIELD COUPLED PROBLEMS: APPLICATION TO THIXOVISCOPLASTIC FLOW

Naheed Begum*, **Abderrahim Ouazzi**, **Stefan Turek**

Institute for Applied Mathematics, LSIII, TU Dortmund University, D-44227 Dortmund, Germany
**corrresponding author*: Naheed.Begum@math.tu-dortmund.de,
Abderrahim.Ouazzi@math.tu-dortmund.de,
Stefan.Turek@math.tu-dortmund.de.

Key words: Finite Element Methods (FEM), Monolithic Newton-Multigrid, Multifield Coupled Problems, Thixoviscoplastic Flow

Abstract. In this note, we are concerned with the solvability of multifield coupled problems with different, often conflictual types of non-linearities. We bring into focus the challenges of getting EFM numerical solutions. As for instance, we share our investigations of the solvability of thixoviscoplastic flow problems in FEM settings. On one hand, nonlinear multifield coupled problems are often lacking unified FEM analysis due to the presence of different non-linearities. Thus, the importance of treating auxiliary subproblems with different analysis tools to guarantee existence of solutions. Moreover, the nonlinear multifield problems are extremely sensitive to the coupling. On other hand, monolithic Newton-multigrid FEM solver shows a great success in getting numerical solutions for multifield coupled problems. Thixoviscoplastic flow problem is a perfect example in this regard. It is a two field coupled problem, by means of microstructure dependent plastic-viscosity as well as microstructure dependent yield stress, and microstructure and shear rate dependent buildup and breakdown functions. We adapt different numerical techniques to show the solvability of the problem, and expose the accuracy of FEM numerical solutions via the simulations of thixoviscoplastic flow problems in channel configuration.

1 Introduction

We shall consider the FEM solvability of multifield nonlinear coupled saddle-point problem of the following system:

Find $(\boldsymbol{u}, p, \lambda) \in \mathbb{V} \times \mathbb{Q} \times \mathbb{T}$, *such that*

$$\begin{cases} \mathcal{A}_{\boldsymbol{u}}(\boldsymbol{u},\lambda)\boldsymbol{u} + \mathcal{B}^{\mathrm{T}} p = l_{\boldsymbol{u}} & \text{in } \mathbb{V}', \\ \mathcal{B}\boldsymbol{u} = 0 & \text{in } \mathbb{Q}', \\ \mathcal{A}_{\lambda}(\boldsymbol{u},\lambda)\lambda = l_{\lambda} & \text{in } \mathbb{T}', \end{cases} \tag{1}$$

or more precisely of the following form:

Find $(\boldsymbol{u}, p, \lambda) \in \mathbb{V} \times \mathbb{Q} \times \mathbb{T}$, *such that*

$$\begin{cases} \mathcal{L}_{\boldsymbol{u}}(\boldsymbol{u},\lambda)\boldsymbol{u} + \mathcal{N}_{\boldsymbol{u}}(\boldsymbol{u})\boldsymbol{u} + \mathcal{B}^{\mathrm{T}}p & = \ l_{\boldsymbol{u}} \qquad \text{in } \mathbb{V}', \\ \mathcal{B}\boldsymbol{u} & = \ 0 \qquad \text{in } \mathbb{Q}', \\ \mathcal{M}_\lambda(\boldsymbol{u},\lambda)\lambda + \mathcal{N}_\lambda(\boldsymbol{u})\lambda & = \ l_\lambda \qquad \text{in } \mathbb{T}', \end{cases} \tag{2}$$

where the operators $\mathcal{A}_{\boldsymbol{u}}, \mathcal{L}_{\boldsymbol{u}} : \mathbb{V}\times\mathbb{T}\times\mathbb{V} \longrightarrow \mathbb{V}'$, $\mathcal{N}_{\boldsymbol{u}} : \mathbb{V}\times\mathbb{V} \longrightarrow \mathbb{V}'$, $\mathcal{A}_\lambda, \mathcal{M}_\lambda : \mathbb{V}\times\mathbb{T}\times\mathbb{T} \longrightarrow \mathbb{T}'$, $\mathcal{N}_\lambda : \mathbb{V}\times\mathbb{T} \longrightarrow \mathbb{T}'$, and the linear forms $\mathcal{B} : \mathbb{V} \longrightarrow \mathbb{Q}'$, $l_{\boldsymbol{u}} : \mathbb{V} \longrightarrow \mathbb{R}$, and $l_\lambda : \mathbb{T} \longrightarrow \mathbb{R}$ are bounded.

The problems (1, 2) are coupled via $(\boldsymbol{u}, p)$ and $(\boldsymbol{u}, \lambda)$, and present different types of nonlinearities. The operator $\mathcal{A}_{\boldsymbol{u}}$ includes two types of nonlinearities via the nonlinear operator $\mathcal{L}_{\boldsymbol{u}}$ and $\mathcal{N}_{\boldsymbol{u}}$, while the operator $\mathcal{A}_\lambda$ induces further nonlinearity via the operator $\mathcal{M}_\lambda$. There is no unified analysis for handling the solvability of the coupled problem $\mathcal{A}_{(\boldsymbol{u},\lambda)}$.

We aim to adapt different analysis tools to show the solvability of nonlinear multifield coupled problems, and present a FEM numerical solutions via the numerical simulations of thixoviscoplastic flow problem.

The problem (1, 2) arise from the quasi-Newtonian modelling approach of Houška thixoviscoplstic model [7, 9]:

$$\begin{cases} \left(\dfrac{\partial}{\partial t} + u\cdot\nabla\right)\boldsymbol{u} - \boldsymbol{\nabla}\cdot\Big(2\mu(D_{\mathbb{I},r},\lambda)\mathbf{D}(\boldsymbol{u})\Big) + \nabla p = \boldsymbol{f}_{\boldsymbol{u}}, \\ \nabla\cdot\boldsymbol{u} = 0, \\ \left(\dfrac{\partial}{\partial t} + u\cdot\nabla\right)\lambda - \mathcal{F}(D_{\mathbb{I},r},\lambda) + \mathcal{G}(D_{\mathbb{I},r},\lambda) = f_\lambda, \end{cases} \tag{3}$$

in Ω, with external forces $\boldsymbol{f}_{\boldsymbol{u}}$, and f_λ. The boundary $\partial\Omega$ might have an inflow Γ^-, outflow section Γ^+ sections, and $\Gamma = \Gamma^- \cup \Gamma^+$. $\boldsymbol{u}$, p, and λ denote velocity, pressure, and microstructure, respectively. The full set of thixoviscoplastic of equations (3) constitute of incompressible viscoplastic equations supplemented with the evolution equation which induces the competition process of *Aging* and *Rejuvenation*. In quasi-Newtonian modelling approach, that we are considering, the viscosity $\mu(\cdot,\cdot)$, breakdown $\mathcal{F}(\cdot,\cdot)$, buildup $\mathcal{G}(\cdot,\cdot)$ functions are dependent on shear rate approximation, $D_{\mathbb{I},r}$, and microstructure λ [9]. We use Papanastasiuo approximation for Forbenius norm of symmetric part of velocity gradient [12]. In Table 1, we list a few thixotropic models.

Table 1: Thixotropic models.

	η	τ	$\mathcal{F}$	$\mathcal{G}$
Worrall et al. [13]	$\lambda\,\eta_0$	τ_0	$\mathcal{M}_a(1-\lambda)\,\lVert\mathbf{D}\rVert$	$\mathcal{M}_b\lambda\,\lVert\mathbf{D}\rVert$
Coussot et al.[5]	$\lambda^g\,\eta_0$		$\mathcal{M}_a$	$\mathcal{M}_b\lambda\,\lVert\mathbf{D}\rVert$
Houška [7]	$(\eta_0+\eta_\infty\lambda)\,\lVert\mathbf{D}\rVert^{n-1}$	$(\tau_0+\tau_\infty\lambda)$	$\mathcal{M}_a(1-\lambda)$	$\mathcal{M}_b\lambda^m\,\lVert\mathbf{D}\rVert$

Here η_0 and τ_0 are initial plastic viscosity and yield stress, respectively. η_∞ and τ_∞ are thixotropic plastic viscosity and yield stress. $\mathcal{M}_a$ and $\mathcal{M}_b$ are buildup and breakage constants, and g, p, m, n are rate indices.

We set the spaces $\mathbb{V} := (H_0^1(\Omega))^2$, $\mathbb{Q} := L_0^2(\Omega)$, and $\mathbb{T} := H^1(\Omega)$, associated with the corresponding norms H^1-norm $\|\cdot\|_1$ and L^2-norm $\|\cdot\|_0$, respectively, $\mathbb{V}'$, $\mathbb{Q}'$, and $\mathbb{T}'$ are their corresponding dual spaces, respectively [2, 3, 6]. We introduce the strong operators $\mathcal{A}_{\boldsymbol{u}}, \mathcal{L}_{\boldsymbol{u}} : \mathbb{V} \times \mathbb{T} \times \mathbb{V} \longrightarrow \mathbb{V}'$, and $\mathcal{N}_{\boldsymbol{u}} : \mathbb{V} \times \mathbb{V} \longrightarrow \mathbb{V}'$ as follows:

$$\langle \mathcal{L}_{\boldsymbol{u}}(\boldsymbol{u}, \lambda)\boldsymbol{u}, \boldsymbol{v}\rangle = \int_\Omega 2\mu(D_{\mathbb{I},r}, \lambda)\mathbf{D}(\boldsymbol{u}) : \mathbf{D}(\boldsymbol{v})\, dx \qquad \forall \boldsymbol{u}, \boldsymbol{v} \in \mathbb{V}, \lambda \in \mathbb{T}, \tag{4}$$

$$\langle \mathcal{N}_{\boldsymbol{u}}(\boldsymbol{w})\boldsymbol{u}, \boldsymbol{v}\rangle = \int_\Omega \boldsymbol{w} \cdot \nabla \boldsymbol{u}\, \boldsymbol{v}\, dx \qquad \forall \boldsymbol{u}, \boldsymbol{v}, \boldsymbol{w} \in \mathbb{V}, \tag{5}$$

and set

$$\mathcal{A}_{\boldsymbol{u}}(\boldsymbol{u}, \lambda) := \mathcal{N}_{\boldsymbol{u}}(\boldsymbol{u}) + \mathcal{L}_{\boldsymbol{u}}(\boldsymbol{u}, \lambda). \tag{6}$$

The operators $\mathcal{A}_\lambda, \mathcal{M}_\lambda : \mathbb{V} \times \mathbb{T} \longrightarrow \mathbb{T}'$, and $\mathcal{N}_\lambda : \mathbb{V} \times \mathbb{T} \longrightarrow \mathbb{T}'$ are defined as follows:

$$\langle \mathcal{M}_\lambda(\boldsymbol{u}, \lambda), \xi\rangle = \int_\Omega \Big(- \mathcal{F}(D_{\mathbb{I},r}, \lambda) + \mathcal{G}(D_{\mathbb{I},r}, \lambda)\Big)\xi\, d\Omega \qquad \forall \lambda, \xi \in \mathbb{T}, \boldsymbol{u} \in \mathbb{V}, \tag{7}$$

$$\langle \mathcal{N}_\lambda(\boldsymbol{u})\lambda, \xi\rangle = \int_\Omega \boldsymbol{u} \cdot \nabla \lambda\, \xi\, dx \qquad \forall \lambda, \xi \in \mathbb{T}, \boldsymbol{u} \in \mathbb{V}, \tag{8}$$

and set

$$\mathcal{A}_\lambda(\boldsymbol{u}, \lambda) := \mathcal{N}_\lambda(\boldsymbol{u}) + \mathcal{M}_\lambda(\boldsymbol{u}, \lambda). \tag{9}$$

The linear forms $\mathcal{B} : \mathbb{V} \longrightarrow \mathbb{Q}'$, $l_{\boldsymbol{u}} : \mathbb{V} \longrightarrow \mathbb{R}$, and $l_\lambda : \mathbb{T} \longrightarrow \mathbb{R}$ are defined as follows:

$$\langle \mathcal{B}\boldsymbol{u}, q\rangle = -\int_\Omega \nabla \cdot \boldsymbol{u}\, q\, dx \qquad \forall \boldsymbol{u} \in \mathbb{V}, q \in \mathbb{Q}, \tag{10}$$

$$l_{\boldsymbol{u}}(\boldsymbol{v}) = \int_\Omega \boldsymbol{f}_{\boldsymbol{u}} \boldsymbol{v}\, dx \qquad \forall \boldsymbol{v} \in \mathbb{V}, \tag{11}$$

$$l_\lambda(\xi) = \int_\Omega f_\lambda\, \xi\, dx \qquad \forall \xi \in \mathbb{T}, \tag{12}$$

The weak formulation for thixoviscoplastic flow problems (3) is described by the system:

Find $(\boldsymbol{u}, p, \lambda) \in \mathbb{V} \times \mathbb{Q} \times \mathbb{T}$, such that

$$\begin{cases} a_{\boldsymbol{u}}(\boldsymbol{u}, \lambda)(\boldsymbol{u}, \boldsymbol{v}) + b(\boldsymbol{v}, p) = \; l_{\boldsymbol{u}}(\boldsymbol{v}) & \forall\, \boldsymbol{v} \in \mathbb{V}, \\ b(\boldsymbol{u}, q) \qquad\qquad\qquad\quad = \; 0 & \forall\, q \in \mathbb{Q}, \\ a_\lambda(\boldsymbol{u}, \lambda)(\lambda, \xi) \qquad\quad\;\; = \; l_\lambda(\xi) & \forall\, \xi \in \mathbb{T}, \end{cases} \tag{13}$$

where, the operators $a_{\boldsymbol{u}}(\boldsymbol{u}, \lambda)(\cdot, \cdot)$, $a_\lambda(\boldsymbol{u}, \lambda)(\cdot, \cdot)$, and $b(\cdot, \cdot)$, given as follows:

$$a_{\boldsymbol{u}}(\boldsymbol{u}, \lambda)(\boldsymbol{u}, \boldsymbol{v}) = \langle \mathcal{A}_{\boldsymbol{u}}(\boldsymbol{u}, \lambda)\boldsymbol{u}, \boldsymbol{v}\rangle \qquad \forall \boldsymbol{u}, \boldsymbol{v} \in \mathbb{V}, \lambda \in \mathbb{T}, \tag{14}$$

$$a_\lambda(\boldsymbol{u}, \lambda)(\lambda, \xi) = \langle \mathcal{A}_\lambda(\boldsymbol{u}, \lambda)\lambda, \xi\rangle \qquad \forall \boldsymbol{u} \in \mathbb{V}, \lambda, \xi \in \mathbb{T}, \tag{15}$$

$$b(\boldsymbol{v}, q) = \langle \mathcal{B}\boldsymbol{v}, q\rangle \qquad \forall \boldsymbol{u}, \boldsymbol{v} \in \mathbb{V}, q \in \mathbb{Q}. \tag{16}$$

We proceed with the corresponding results for existence and uniqueness of the solutions for coupled nonlinear multifield problems (1, 2).

2 Theoretical results

Here we make use of each and every operator property to establish the wellposedness of nonlinear multified coupled problems (1). As for instance, the operator $\mathcal{L}_{\boldsymbol{u}}$ is monotone, $\mathcal{N}_{\boldsymbol{u}}$ is only coercive, $\mathcal{M}_\lambda$ is not coercive in the complete norm. With the definitions of the operators $\mathcal{L}_{\boldsymbol{u}}$, $\mathcal{N}_{\boldsymbol{u}}$, $\mathcal{M}_\lambda$, and $\mathcal{N}_\lambda$, and the embedding property of H^1 in L^4, we show the boundedness of all operators, that is there are positive constants $\|\mathcal{L}_{\boldsymbol{u}}\|$, $\|\mathcal{N}_{\boldsymbol{u}}\|$, $\|\mathcal{M}_\lambda\|$, and $\|\mathcal{N}_\lambda\|$ such that

$$|\langle \mathcal{L}_{\boldsymbol{u}}(\boldsymbol{u},\lambda)\boldsymbol{w},\boldsymbol{v}\rangle| \leq \|\mathcal{L}_{\boldsymbol{u}}\| \, \|\boldsymbol{w}\|_{\mathbb{V}} \, \|\boldsymbol{v}\|_{\mathbb{V}} \qquad \forall \boldsymbol{u},\boldsymbol{v},\boldsymbol{w} \in \mathbb{V}, \lambda \in \mathbb{T}, \tag{17}$$
$$|\langle \mathcal{N}_{\boldsymbol{u}}(\boldsymbol{u})\boldsymbol{w},\boldsymbol{v}\rangle| \leq \|\mathcal{N}_{\boldsymbol{u}}\| \, \|\boldsymbol{u}\|_{\mathbb{V}} \, \|\boldsymbol{w}\|_{\mathbb{V}} \, \|\boldsymbol{v}\|_{\mathbb{V}} \qquad \forall \boldsymbol{u},\boldsymbol{v},\boldsymbol{w} \in \mathbb{V}, \tag{18}$$
$$|\langle \mathcal{M}_\lambda(\boldsymbol{u},\lambda),\xi\rangle| \leq \|\mathcal{M}_\lambda\| \, \|\boldsymbol{u}\|_{\mathbb{V}} \, \|\lambda\|_{\mathbb{T}} \, \|\xi\|_{\mathbb{T}} \qquad \forall \boldsymbol{u},\lambda,\xi \in \mathbb{T}, \tag{19}$$
$$|\langle \mathcal{N}_\lambda(\boldsymbol{u})\lambda,\xi\rangle| \leq \|\mathcal{N}_\lambda\| \, \|\boldsymbol{u}\|_{\mathbb{V}} \, \|\lambda\|_{\mathbb{T}} \, \|\xi\|_{\mathbb{T}} \qquad \forall \boldsymbol{u},\lambda,\xi \in \mathbb{T}. \tag{20}$$

Also, the boundedness of linear form $\mathcal{B}$, and the linear functionals $l_{\boldsymbol{u}}$, and l_λ

$$|\langle \mathcal{B}\boldsymbol{v},q\rangle| \leq \|\mathcal{B}\| \, \|\boldsymbol{v}\|_{\mathbb{V}} \, \|q\|_{\mathbb{Q}} \qquad \forall \boldsymbol{v} \in \mathbb{V},\, q \in \mathbb{Q}, \tag{21}$$
$$|l_{\boldsymbol{u}}(\boldsymbol{v})| \leq \|l_{\boldsymbol{u}}\| \, \|\boldsymbol{v}\|_{\mathbb{V}} \qquad \forall \boldsymbol{v} \in \mathbb{V}, \tag{22}$$
$$|l_\lambda(\xi)| \leq \|l_\lambda\| \, \|\xi\|_{\mathbb{T}} \qquad \forall \xi \in \mathbb{T}. \tag{23}$$

We introduce the space $\mathbb{V}_0 := \ker \mathcal{B}$ of strongly divergence-free velocity

$$\mathbb{V}_0 = \{\boldsymbol{v} \in \mathbb{V} \mid \mathcal{B}\boldsymbol{v} = 0\}\,. \tag{24}$$

Now, we proceed with the boundedness from below of the operators $\mathcal{L}_{\boldsymbol{u}}$, $\mathcal{M}_\lambda$, and $\mathcal{N}_\lambda$.

$$|\langle \mathcal{L}_{\boldsymbol{u}}(\boldsymbol{v},\lambda)\boldsymbol{v},\boldsymbol{v}\rangle| \geq \eta_0 \mathcal{C}_K \|\boldsymbol{v}\|_{\mathbb{V}}^2 \qquad \forall \boldsymbol{v} \in \mathbb{V}_0, \lambda \in \mathbb{T}, \tag{25}$$
$$|\langle \mathcal{M}_\lambda(\boldsymbol{v},\xi),\xi\rangle| \geq \mathcal{M}_a \|\xi\|_0^2 \qquad \forall \boldsymbol{v} \in \mathbb{V}_0, \xi \in \mathbb{T}, \tag{26}$$
$$|\langle \mathcal{N}_\lambda(\boldsymbol{v}),\xi\rangle| \geq \frac{1}{2}\langle |\boldsymbol{v}\cdot\boldsymbol{n}|\,\xi\rangle_\Gamma^2 \qquad \forall \boldsymbol{v} \in \mathbb{V}_0, \xi \in \mathbb{T}, \tag{27}$$

where, $\mathcal{C}_K$ denotes Korn's inequality constant in (25), and the right hand side of (27) is the boundary norm.
We start by defining the operator

$$\tilde{\mathcal{A}}_{\boldsymbol{u}} := \mathcal{L}_{\boldsymbol{u}}(\boldsymbol{u},\lambda) + \mathcal{N}_{\boldsymbol{u}}(\boldsymbol{w}), \quad \forall (\boldsymbol{w},\lambda) \in \mathbb{V}_0 \times \mathbb{T}. \tag{28}$$

and consider the problem:

Find $\boldsymbol{u} \in \mathbb{V}_0$, such that

$$\langle \tilde{\mathcal{A}}_{\boldsymbol{u}}\boldsymbol{u},\boldsymbol{v}\rangle = \langle\, l_{\boldsymbol{u}},\boldsymbol{v}\rangle, \quad \forall \boldsymbol{v} \in \mathbb{V}_0. \tag{29}$$

Then, let $\boldsymbol{u},\boldsymbol{v} \in \mathbb{V}_0$, and set $\boldsymbol{\eta} = \boldsymbol{u} - \boldsymbol{v}$, we use the monotonicity of the plastic part of the operator $\mathcal{L}_{\boldsymbol{u}}$ ([3]), and first Korn's inequality to get

$$\langle \mathcal{L}_{\boldsymbol{u}}(\boldsymbol{u},\lambda)\boldsymbol{u},\boldsymbol{\eta}\rangle - \langle \mathcal{L}_{\boldsymbol{u}}(\boldsymbol{v},\lambda)\boldsymbol{v},\boldsymbol{\eta}\rangle \geq \; \eta_0 \mathcal{C}_K \|\boldsymbol{\eta}\|_{\mathbb{V}}^2 \quad \forall \boldsymbol{u},\boldsymbol{v},\boldsymbol{\eta} \in \mathbb{V}_0, \tag{30}$$

and the following property of the operator $\mathcal{N}_{\boldsymbol{u}}$

$$\langle \mathcal{N}_{\boldsymbol{u}}(\boldsymbol{w})\boldsymbol{\eta},\boldsymbol{\eta}\rangle = 0 \quad \forall \boldsymbol{w},\boldsymbol{\eta} \in \mathbb{V}_0, \tag{31}$$

to deduce the monotonicity of the operator $\tilde{\mathcal{A}}_{\boldsymbol{u}}$. With the boundedness the operators $\mathcal{L}_{\boldsymbol{u}}$ from (17), and the operator $\mathcal{N}_{\boldsymbol{u}}$ from (18), we conclude the existence and uniqueness of solution of $\boldsymbol{u} = \boldsymbol{u}(\boldsymbol{w}, \lambda)$ of the problem (29). Furthermore, the solutions are bounded

$$\|\boldsymbol{u}(\boldsymbol{w}, \lambda)\|_{\mathbb{V}} \leq \frac{1}{\eta_0 \mathcal{C}_K} \|l_{\boldsymbol{u}}\| . \tag{32}$$

Thus, the mapping $\boldsymbol{w} \mapsto \tilde{\mathcal{A}}_{\boldsymbol{u}}(\boldsymbol{w})$ is invertible, and locally Lipschitz continuous in $\mathbb{V}_0$, that is

$$\left|\tilde{\mathcal{A}}_{\boldsymbol{u}}(\boldsymbol{u}) - \tilde{\mathcal{A}}_{\boldsymbol{u}}(\boldsymbol{v})\right| \leq \|\mathcal{N}_{\boldsymbol{u}}\| \, \|\boldsymbol{u} - \boldsymbol{v}\|_{\mathbb{V}} \quad \forall \boldsymbol{u}, \boldsymbol{v} \in \mathbb{V}_0. \tag{33}$$

Furthermore, the invertible operator $\tilde{\mathcal{A}}_{\boldsymbol{u}}^{-1}(\boldsymbol{w})$ is bounded in $\mathcal{L}(\mathbb{V}_0', \mathbb{V}_0)$

$$\left\|\tilde{\mathcal{A}}_{\boldsymbol{u}}^{-1}(\boldsymbol{w})\right\| := \left\|\tilde{\mathcal{A}}_{\boldsymbol{u}}^{-1}(\boldsymbol{w})\right\|_{\mathcal{L}(\mathbb{V}_0', \mathbb{V}_0)} \leq \frac{1}{\eta_0 \mathcal{C}_K}. \tag{34}$$

We introduce the space of bounded solution

$$\mathcal{BS}_{\mathcal{A}_{\boldsymbol{u}}} = \left\{ \boldsymbol{u} \in \mathbb{V}_0 \mid \|\boldsymbol{u}\|_{\mathbb{V}} \leq \frac{1}{\eta_0 \mathcal{C}_K} \|l_{\boldsymbol{u}}\| \right\}. \tag{35}$$

In order to utilize fixed point theorem for the mapping $\boldsymbol{w} \mapsto \tilde{\mathcal{A}}_{\boldsymbol{u}}^{-1}(\boldsymbol{w})$, we show the contraction property of the operator $\tilde{\mathcal{A}}_{\boldsymbol{u}}^{-1}$, that is

$$\left|\tilde{\mathcal{A}}_{\boldsymbol{u}}^{-1}(\boldsymbol{u}) l_{\boldsymbol{u}} - \tilde{\mathcal{A}}_{\boldsymbol{u}}^{-1}(\boldsymbol{v}) l_{\boldsymbol{u}}\right| \leq \|\mathcal{N}_{\boldsymbol{u}}\| \frac{1}{(\eta_0 \mathcal{C}_K)^2} \|l_{\boldsymbol{u}}\| \, \|\boldsymbol{u} - \boldsymbol{v}\|_{\mathbb{V}} \quad \forall \boldsymbol{u}, \boldsymbol{v} \in \mathcal{BS}_{\mathcal{A}_{\boldsymbol{u}}}, \tag{36}$$

where, we used the locally Lipschitz continuous property (33), and assumed that

$$\|\mathcal{N}_{\boldsymbol{u}}\| \frac{1}{(\eta_0 \mathcal{C}_K)^2} \|l_{\boldsymbol{u}}\| < 1. \tag{37}$$

We conclude the existence and uniqueness of solution $\boldsymbol{u}(\lambda) \in \mathbb{V}_0$, $\forall \lambda \in \mathbb{T}$ of the $\boldsymbol{u}$-field subproblem:

Find $\boldsymbol{u} \in \mathbb{V}_0$, such that

$$\langle \mathcal{A}_{\boldsymbol{u}} \boldsymbol{u}, \boldsymbol{v} \rangle = \langle \, l_{\boldsymbol{u}}, \boldsymbol{v} \rangle, \quad \forall \boldsymbol{v} \in \mathbb{V}_0, \lambda \in \mathbb{T}. \tag{38}$$

In parallel we show the existence and uniqueness of the microstructure subproblem, before establishing the solvability of the nonlinear multifield coupled problem. To do so, we just apply Lax-Milgram Theorem. We show the coercivity of $\mathcal{A}_\lambda$ from (26) and (27), beside the continuity of $\mathcal{A}_\lambda$ from (19), and (20) , and the boundedness of l_λ from (23), and deduce the existence and uniqueness of solution λ of the λ-field subproblem

$$\mathcal{A}_\lambda(\boldsymbol{u}, \lambda)\lambda = l_\lambda \quad \forall \boldsymbol{u} \in \mathbb{V}_0. \tag{39}$$

Moreover, the solution is bounded ([3])

$$\mathcal{M}_a \|\lambda\|_0^2 + \frac{1}{2} \langle |\boldsymbol{u} \cdot \boldsymbol{n}| \, \lambda \rangle_\Gamma^2 \leq \frac{1}{\mathcal{M}_a} \|l_\lambda\| . \tag{40}$$

We denote by $\mathcal{BS}_{\mathcal{A}_\lambda}$ the space of microstructure bounded solutions for a given $\boldsymbol{u} \in \mathbb{V}_0$, that is

$$\mathcal{BS}_{\mathcal{A}_\lambda} = \left\{ \lambda \in \mathbb{T} \mid \mathcal{M}_a \left\|\lambda\right\|_0^2 + \frac{1}{2}\langle |\boldsymbol{u}\cdot\boldsymbol{n}|\, \lambda\rangle_\Gamma^2 \leq \frac{1}{\mathcal{M}_a}\left\|l_\lambda\right\| \right\}. \tag{41}$$

We introduce the space of bounded coupled solutions

$$\mathcal{BS}_{\mathcal{A}_{(\boldsymbol{u},\lambda)}} := \mathcal{BS}_{\mathcal{A}_{\boldsymbol{u}}} \times \mathcal{BS}_{\mathcal{A}_\lambda}. \tag{42}$$

Now, we proceed to show the existence and uniqueness of the solution for the coupled problem. We check the continuity property, let $(\boldsymbol{u},\lambda), (\boldsymbol{v},\xi), \tilde{\boldsymbol{\eta}} = (\boldsymbol{\eta},\zeta) \in \mathbb{V}_0 \times \mathbb{T}$, and assume the necessary regularity requirement, we have

$$\begin{aligned}
\langle \mathcal{A}_{\boldsymbol{u}}(\boldsymbol{u},\lambda)\boldsymbol{u},\boldsymbol{\eta}\rangle - \langle \mathcal{A}_{\boldsymbol{u}}(\boldsymbol{v},\xi)\boldsymbol{v},\boldsymbol{\eta}\rangle \leq & \Big((2\eta_0 + 2\eta_\infty \left\|\xi\right\|_0) \\
& + (2\tau_0 + \tau_\infty(\left\|\lambda\right\|_0 + \left\|\xi\right\|_0)k\Big) \left\|\boldsymbol{u}-\boldsymbol{v}\right\|_{\mathbb{V}} \left\|\boldsymbol{\eta}\right\|_{\mathbb{V}} \\
& + \Big(\left\|\mathcal{N}_{\boldsymbol{u}}\right\| \left\|\boldsymbol{u}\right\|_{\mathbb{V}} + \left\|\mathcal{N}_{\boldsymbol{u}}\right\| \left\|\boldsymbol{v}\right\|_{\mathbb{V}} \Big) \left\|\boldsymbol{u}-\boldsymbol{v}\right\|_{\mathbb{V}} \left\|\boldsymbol{\eta}\right\|_{\mathbb{V}} \\
& + \Big(2\eta_\infty \left\|\boldsymbol{v}\right\|_{\mathbb{V}} + \tau_\infty k \left\|\boldsymbol{v}\right\|_{\mathbb{V}} \Big) \left\|\lambda-\xi\right\|_{\mathbb{T}} \left\|\boldsymbol{\eta}\right\|_{\mathbb{V}}, \\
\langle \mathcal{A}_\lambda(\boldsymbol{u},\lambda)\lambda,\zeta\rangle - \langle \mathcal{A}_\lambda(\boldsymbol{v},\xi)\xi,\zeta\rangle \leq & \Big(\mathcal{M}_b + 1 \Big) \left\|\boldsymbol{u}\right\|_{\mathbb{V}} \left\|\lambda-\xi\right\|_{\mathbb{T}} \left\|\zeta\right\|_{\mathbb{T}} \\
& + \langle |\boldsymbol{u}\cdot\boldsymbol{n}|\, \lambda-\xi\rangle_{\Gamma^+} \left\|\zeta\right\|_{\mathbb{T}} \\
& + \Big(\mathcal{M}_b + 1 \Big) \left\|\xi\right\|_0 \left\|\boldsymbol{u}-\boldsymbol{v}\right\|_{\mathbb{V}} \left\|\zeta\right\|_{\mathbb{T}} \\
& + \langle |(\boldsymbol{u}-\boldsymbol{v})\cdot\boldsymbol{n}|\, \xi\rangle_{\Gamma^+} \left\|\zeta\right\|_{\mathbb{T}}.
\end{aligned} \tag{43}$$

We consider the mapping $\mathcal{A}_{(\boldsymbol{u},\lambda)} : \mathcal{BS}_{\mathcal{A}_{(\boldsymbol{u},\lambda)}} \mapsto \mathcal{BS}_{\mathcal{A}_{(\boldsymbol{u},\lambda)}}$, which we rewrite as follows:

$$\mathcal{A}_{(\boldsymbol{u},\lambda)} = \bar{\bar{\mathcal{A}}}_{(\boldsymbol{u},\lambda)} + \mathcal{A}_{(\boldsymbol{u},0)}, \tag{44}$$

with $\mathcal{A}_{(\boldsymbol{u},0)}$ is nonthixotropic viscoplastic operator which is completely continuous, and $\bar{\bar{\mathcal{A}}}_{(\boldsymbol{u},\lambda)}$ is nonlinear contraction [4, 8], that is

$$\left| \bar{\bar{\mathcal{A}}}_{(\boldsymbol{u},\lambda)}(\boldsymbol{u},\lambda) - \bar{\bar{\mathcal{A}}}_{(\boldsymbol{u},\lambda)}(\boldsymbol{v},\xi) \right| \leq \phi\Big((\left\|\boldsymbol{u}-\boldsymbol{v}\right\|_{\mathbb{V}}^2 + \left\|\lambda-\xi\right\|_{\mathbb{T}}^2)^{\frac{1}{2}} \Big) \tag{45}$$

where ϕ is real valued continuous function such that

$$\phi(0) = 0, \text{ and } \phi(r) < r \text{ for } r > 0. \tag{46}$$

The inequality (45) is due to the continuity property (43), its implicit expression is simply due the boundedness of microstructure with the boundary norm. Thus, the nonlinear multified coupled problem admits a solution. The existence of the pressure is due to the well known Lagrange multiplier argument.

3 Numerical Results

For the numerical results, we use a corresponding developed monolithic Newton-multigrid FEM solver, we refer to [1, 11] for more details. The solver uses Local pressure Schur complement approach to solve the coupled problem locally and update the global solution via block Gauss-Seidel iteration, this element-wise treatment is advantageously exploited, on one hand by using linear *discountinuous* pressure P_1^{disc}, and on other hand by collocating the velocity and microstructure in quadratic interpolation Q_2 [10]. The nonlinear discrete system is solver using adaptive discrete Newton's method, and the linear systems are solved with multigrid method. We use a unit channel configuration for thixoviscoplastic flow simulations. We use the fully developed flow assumption to develop a reduced one-dimensional Houška thixoviscoplastic model to generate the flow profile for the boundary conditions of two-dimensional FEM simulations. On one hand, we use the reduced one-dimensional flow profiles as Dirichlet boundary conditions at inflow for both velocity and microstructure. On other hand, instead of using the well-known 'do-nothing' boundary condition at outflow, we use the reduced one-dimensional flow profiles as Dirichlet boundary conditions. Moreover, we use the one-dimensional flow profiles as validation tools for the fully developed flow assumption, that is the accuracy of the two-dimensional FEM solutions.

In Figure 1, we present the comparison of one-dimensional reduced Houška model solutions, and the two-dimensional FEM Houška's simulations.

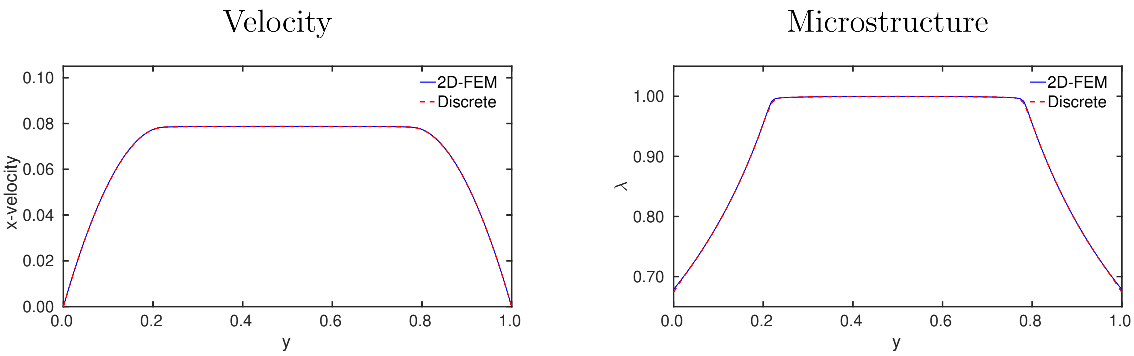

Figure 1: **Fully developed channel flow:** The one-dimensional reduced Houška model solutions versus the two-dimensional FEM Houška's solutions. The two-dimensional FEM solution's profiles are taken at the vertical centerline, $x = 0.5$, of the channel. The model's parameters are set to $\eta_0 = 1.0$, $\eta_\infty = 0.0$, $\tau_0 = 0.0$, $\tau_\infty = 0.25$, $\mathcal{M}_a = \mathcal{M}_b = 0.1$, and $k = 10^4$.

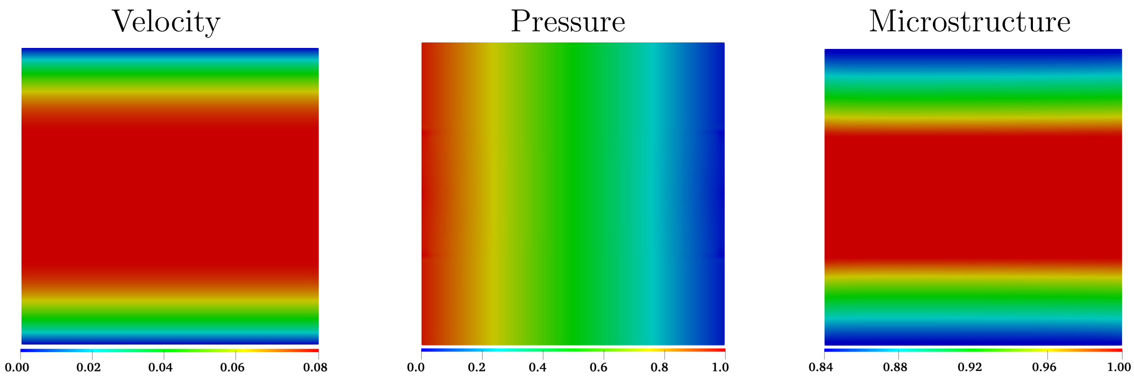

Figure 2: **Fully developed channel flow:** The FEM nonlinear multifield coupled Houška thixoviscoplastic flow distribution. The model's parameters are set to $\eta_0 = 1.0$, $\eta_\infty = 0.0$, $\tau_0 = 0.0$, $\tau_\infty = 0.25$, $\mathcal{M}_a = \mathcal{M}_b = 0.1$, and $k = 10^4$.

From Figure 1, the fully developed flow assumptions are verified at the vertical centerline, $x = 0.5$, as a prototype for each vertical line. Indeed the flow distribution of the two-dimensional FEM Houška's simulations in Figure 2 indicates the accuracy of the solutions, as the flow remains unchanged along the channel, independent of the channel length.

In next simulation, we investigate the microstructure-velocity coupling via the changes of breakdown parameter. In Figure 3, we present the two-dimensional FEM Houška's microstructure's profiles at the channel center for different values of breakdown parameter $\mathcal{M}_b$.

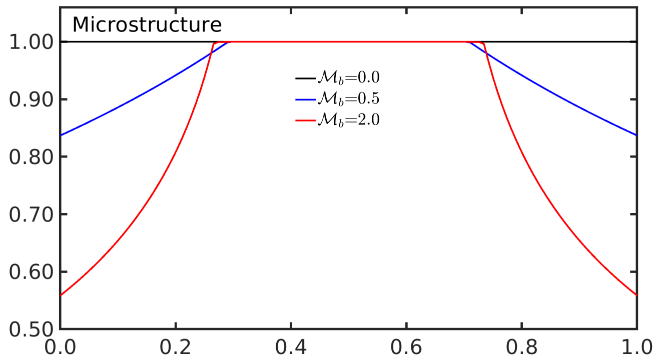

Figure 3: **Fully developed channel flow:** Impact of breakdown parameter $\mathcal{M}_b$ on microstructure solutions. The model's parameters are set to $\eta_0 = 1.0$, $\eta_\infty = 0.0$, $\tau_0 = 0.0$, $\tau_\infty = 0.25$, $\mathcal{M}_a = 0.1$, and $k = 10^4$.

The response of the flow simulations with respect to breakdown parameter is manifested via the microstructure profiles in Figure 3. As, we decrease the breakdown parameter the thixotropic plastic contribution is getting dominant. Moreover, the transitions form the flowing zones and the non-flowing zone are sharper at higher breakdown parameter.

4 Summary

We investigated, for FEM settings, the nonlinear multifield coupled problems from theoretical and numerical perspectives. We used the thixoviscoplastic flow as a motivation example for such type of problems. From theoretical standpoint, we established the solvability of the problem with respect to the properties of its operators constituent. In the start, we made use of monotonicity property of diffusion operator, and fixed point theorem for the complete momentum equation, which integrate the convection nonlinearity, to demonstrate the solvability of the viscoplastic subproblem for any given microstructure. In parallel, the solvabilty of the microstructure subproblem for a given divergence-fee velocity is shown using Lax-Milgram theorem. Then, the coupled multifield operator is rewritten as a sum of completely continuous non-thixotropic viscoplastic operator, and nonlinear contraction thixoviscoplastic operator to make use of a variant of fixed point theorem to demonstrate the solvability of the coupled problem. And from numerical simulations standpoint, we used monolithic Newton-multigrid FEM solver developed for nonlinear multifield coupled problems to simulate thixoviscoplastic flow in channel configuration [1]. In this regards, we made use of fully developed flow assumption to develop a reduced one-dimensional model which we used to generate solutions profiles. The reduced one-dimensional solutions profiles are used as Dirichlet boundary conditions at inflow, alternative to "do-nothing" boundary conditions at outflow, and as validation for the fully developed flow, for two-dimensional FEM flow simulations. The FEM numerical simulations confirmed the accuracy of the solutions of nonlinear multifield coupled problems with respect to both the solver and the boundary conditions settings. Moreover, we analyzed the microstructure-velocity coupling by varying the breakdown parameter, which confirmed the accuracy of the solutions once again as the thixotropic plastic is getting dominant with an increasing breakdown parameters, beside the transitions between the flowing zones and the non-flowing zone are getting sharper at higher breakdown parameter.

Acknowledgement: The authors acknowledge the funding provided by the "Deutsche Forschungsgemeinschaft (DFG, German Research Foundation) - 446888252". We would also like to gratefully acknowledge the support by LSIII and LiDO3 team at ITMC, TU Dortmund University, Germany.

REFERENCES

[1] Begum, N., Ouazzi, A., Turek, S. Efficient Newton-multigrid FEM Solver for Multifield Nonlinear Coupled Problems Applied to Thixoviscoplastic Flows. *Ergebnisberichte des Instituts für Angewandte Mathematik, Nummer 665, Fakultät für Mathematik, TU Dortmund University* ISBN: 2190-1767 (2023).

[2] Begum, N., Ouazzi, A., Turek, S. FEM simulation of thixo–viscoplastic flow problems: Error analysis. *Special Issue: 92nd Annual Meeting of the International Association of Applied Mathematics and Mechanics (GAMM)*, https://doi.org/10.1002/pamm.202200294, Wiley-Interscience 23:1 (2023).

[3] Begum, N., Ouazzi, A., Turek, S. FEM analysis and monolithic Newton-multigrid solver for thixo-viscoplastic flow problems. *ECCOMAS Congress 2022 - 8th European Congress on Computational Methods in Applied Sciences and Engineering, doi.org/10.23967/eccomas.2022.119*, (2022).

[4] Boyd, D. W., Boyd, D. W. On Nonlinear Contractions. *Proceedings of the American Mathematical Society*, 2(20) 458–464, (1969).

[5] Coussot, P., Nguyen, Q. D., Huynh, H. T., Bonn, D. Viscosity bifurcation in thixotropic, yielding fluids. *J. Rheol.* **46**(3):573–589 (2002).

[6] Girault, V., Raviart, P. A. Finite Element Approximation of the Navier Stokes Equations. *Lecture Notes in Mathematics* 749, *Springer Verlag Berlin Heidelberg*, (1979).

[7] Houška, M. *Engineering aspects of the rheology of thixotropic liquids.* PhD thesis, Faculty of Mechanical Engineering, Czech Technical University of Prague, (1981).

[8] Nashed, M. Z. and Wong, J. S. Some Variants of a Fixed Point Theorem of Krasnoselskii and Applications to Nonlinear Integral Equations. *Journal of Mathematics and Mechanics*, 18(8):767–777, (1969).

[9] Ouazzi, A., Begum, N., Turek, S. Newton-Multigrid FEM Solver for the Simulation of Quasi-Newtonian Modeling of Thixotropic Flows. *Numerical Methods and Algorithms in Science and Engineering* 700, (2021).

[10] Ouazzi, A., Turek, S. *Efficient multigrid and data structures for edge-oriented FEM stabilization*, Numerical Mathematics and Advanced Applications Enumath 2005, Springer Berlin Heidelberg, ISBN-10 3-540-34287-7, 520–527 (2006).

[11] Ouazzi, A. *Finite Element Simulation of Nonlinear Fluids. Application to Granular Material and Powder*, Shaker Verlag, Achen (2006).

[12] Papanastasiuo, T. C., Flow of materials with yield. *J. Rheol.*, **31**:385-404 (1987).

[13] Worrall, W. E., Tuliani, S. Viscosity changes during the aging of clay-water suspensions. *Trans. Brit. Ceramic Soc.***63**:167-185 (1964).